nanomaterials

MDPI

Article

Supplementary Materials

Gold Nanorod Assemblies: The Roles of Hot-Spot Positioning and Anisotropy in Plasmon Coupling and SERS

Priyanka Dey [1,2,*,†], Verena Baumann [1,2] and Jessica Rodríguez-Fernández [1,2,‡]

[1] Department of Physics and CeNS, Ludwig-Maximilians-Universität München, Munich 80539, Germany; verena-baumann@gmx.de (V.B.); jessica.rodriguezfdez@gmail.com (J.R.-F.)

[2] Nanosystems Initiative Munich (NIM), Munich 80799, Germany

* Correspondence: p.dey@exeter.ac.uk

† Current affiliation: School of Physics and Astronomy, University of Exeter, Exeter EX4 4QL, UK.

‡ Current affiliation: Wacker Chemie AG, Johannes-Hess-Straße 24, 84489 Burghausen, Germany.

INDEX:

1. Formation of Anisotropic Directional AuNRs@DNA@Ag Building Blocks by Selective DNA Inactivation of AuNRs@DNA

As described in the manuscript, we investigated the epitaxial overgrowth of Ag on AuNRs@DNA by two approaches:

Ag^+ reduction assisted by polyvinylpirrolidone (PVP) and L-sodium ascorbate and

Ag^+ reduction assisted by hydroquinone.

In the following sections, we provide details of both approaches and the justification for the selection of the second one for the formation of well-defined and stable directional AuNRs@DNA@Ag building blocks.

1.1. DNA Inactivation by Ag^+ Reduction Assisted by PVP and L-Sodium Ascorbate

The experimental conditions used to grow Ag on DNA-functionalized AuNRs were conveniently adapted from those reported by Lee *et al.* [1] for spherical AuNPs@DNA, so as to reach in our case a homogeneous octahedral Ag overgrowth. For the results shown in Figure S1 and Figure S2, to 250 μL of AuNRs@PEG-T_{18}-DNA (Au NR length × width = 69 × 18 nm, DNA grafting = 311 strands/AuNR, [Au] = 0.5 mM) redispersed in phosphate buffer containing 3 mM NaCl, a given volume (see below) of an aqueous 0.42 mM $AgNO_3$ solution was added. This was followed by the quick addition of a given volume of an aqueous 0.42% PVP solution (Mw = 10000 g/mol) and of an aqueous 42 mM L-sodium ascorbate (L-SA) solution. The solution mixture was mildly shaken in an orbital shaker, while allowing the reaction to proceed undisturbed at room temperature. In all experiments, the volumes of the reactants were adjusted so that the molar ratio between the number of PVP repeating units and Ag^+ was kept at 30 and the molar ratio LSA/Ag^+ at 50. The final reaction volume was kept constant at 523 μL, with a final [Au] therein of 0.24 mM. The extent of Ag overgrowth and, therefore, of the truncation of the Ag lateral facets, was controlled by adjusting the [Ag^+]/[Au] ratio, as shown in and **Error! Reference source not found.** Figure S2below.

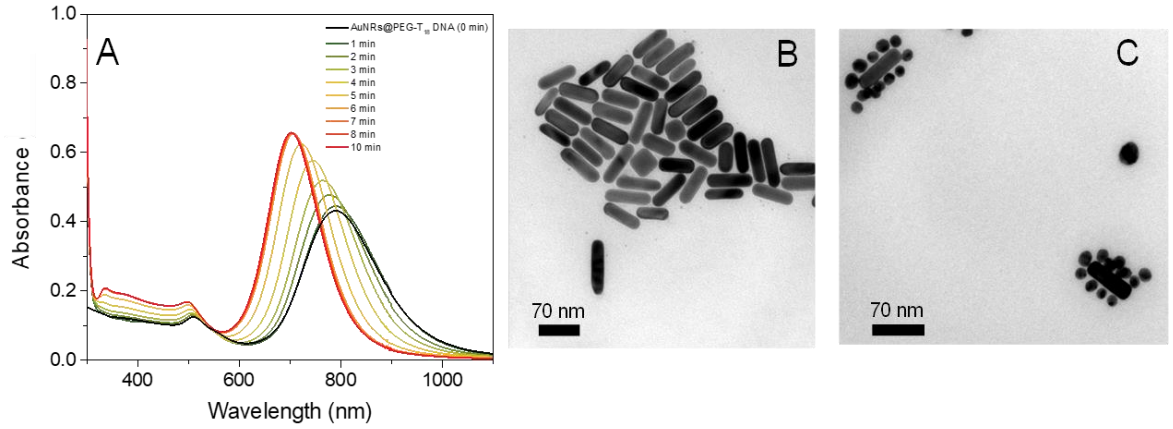

Figure S1. (**A**) Evolution of the UV–vis–NIR spectrum of AuNRs@PEG-T_{18}-DNA upon PVP-assisted Ag deposition at an [Ag^+]/[Au] ratio of 0.5. The reaction was completed within ca. 8 min. (**B**) TEM micrograph of AuNRs@PEG-T_{18}-DNA@Ag obtained at the end of the process. The average Ag thickness at the Au NRs lateral facets was 3 nm. (**C**) TEM micrograph of the nano-assemblies obtained upon incubation of AuNRs@PEG-T_{18}-DNA@Ag shown in (**B**) with a 20-fold excess of 15 nm spherical Au NPs functionalized with complementary DNA strands (AuNPs@A_{18}-DNA). Self-assembly was allowed to proceed overnight at room temperature in the presence of 0.05 M NaCl. The formation of non-directional assemblies appeared in agreement with the fact that the PEG-T_{18}-DNA strands were longer (~20 nm) than the actual Ag coating. This enabled them to be fully available for hybridization with the DNA-functionalized spherical Au NPs, thus leading to non-directional nano-assemblies. However, as shown in Figure S2 below, this non-directional assembly was strongly influenced by the PVP that became grafted on the surface of AuNRs@PEG-T_{18}-DNA@Ag as the Ag deposition proceeded. Therefore, the hybridization capabilities of the DNA strands were significantly hindered by the attractive effect of the polymer towards the spherical Au NPs.

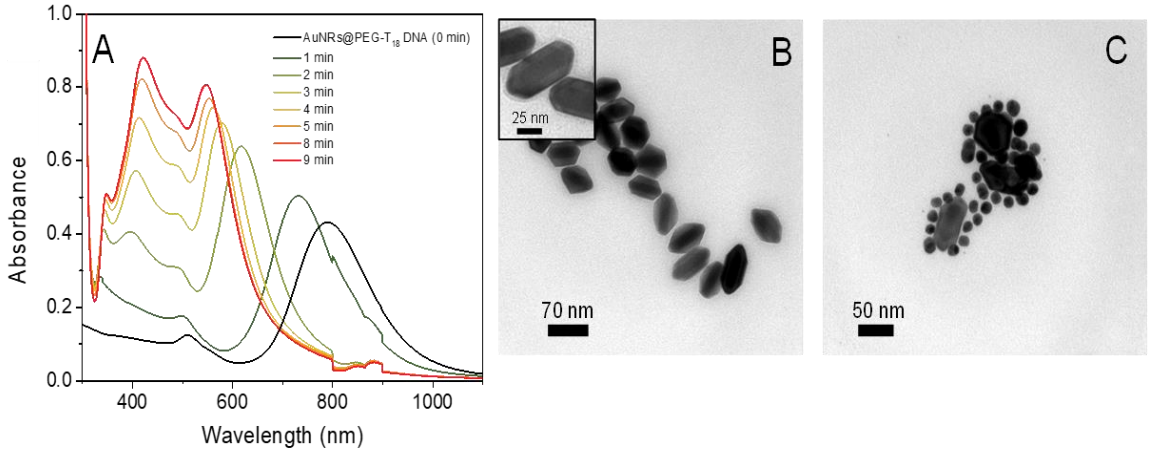

Figure S2. (**A**) UV–vis–NIR spectral evolution of AuNRs@PEG-T_{18}-DNA upon PVP-assisted Ag deposition at a [Ag^+]/[Au] ratio of 3. The reaction was completed within ca. 8 min. (**B**) Representative TEM micrograph of AuNRs@PEG-T_{18}-DNA@Ag obtained at the end of the reaction. The average Ag thickness at the Au NRs lateral facets was 22 nm. Inset: enlargement showing that PVP still remained on the nanoparticles' surface (see halo) in spite of thorough washing. (**C**) TEM micrograph of the nano-assemblies obtained upon incubation of AuNRs@PEG-T_{18}-DNA@Ag shown in (**B**) with a 20-fold excess of 15 nm spherical Au NPs functionalized with complementary DNA strands (AuNPs@A_{18}-DNA). Self-assembly was allowed to proceed overnight at room temperature in the presence of 0.05 M NaCl. The PEG-T_{18}-DNA strands at the lateral facets of Au NRs were fully buried by the 22 nm-thick Ag coating. Therefore, formation of directional nano-assemblies (with AuNPs@A_{18}-DNA selectively self-assembled at the tips and tip region of AuNRs@PEG-T_{18}-DNA@Ag) would be expected. However, the TEM micrograph in (**C**) clearly shows that spherical Au NPs were also self-assembled at the lateral facets. This was due to the interfering effect of the grafted PVP. In spite of thorough washing in several centrifugation/redispersion cycles, the polymer could not be fully removed from the surface of AuNRs@PEG-T_{18}-DNA@Ag (see inset in (**B**)) and, therefore, competed with DNA hybridization.

Due to the interfering role of PVP during assembly, we decided to pursue an alternative, polymer-free method (namely, a hydroquinone-based one) for Ag^+ reduction and epitaxial Ag overgrowth on single-crystal AuNRs@DNA. This method allowed us to selectively impose directional interactions on AuNRs@DNA@Ag, as shown and discussed in the manuscript.

1.2. DNA Inactivation by Ag^+ Reduction Assisted by Hydroquinone

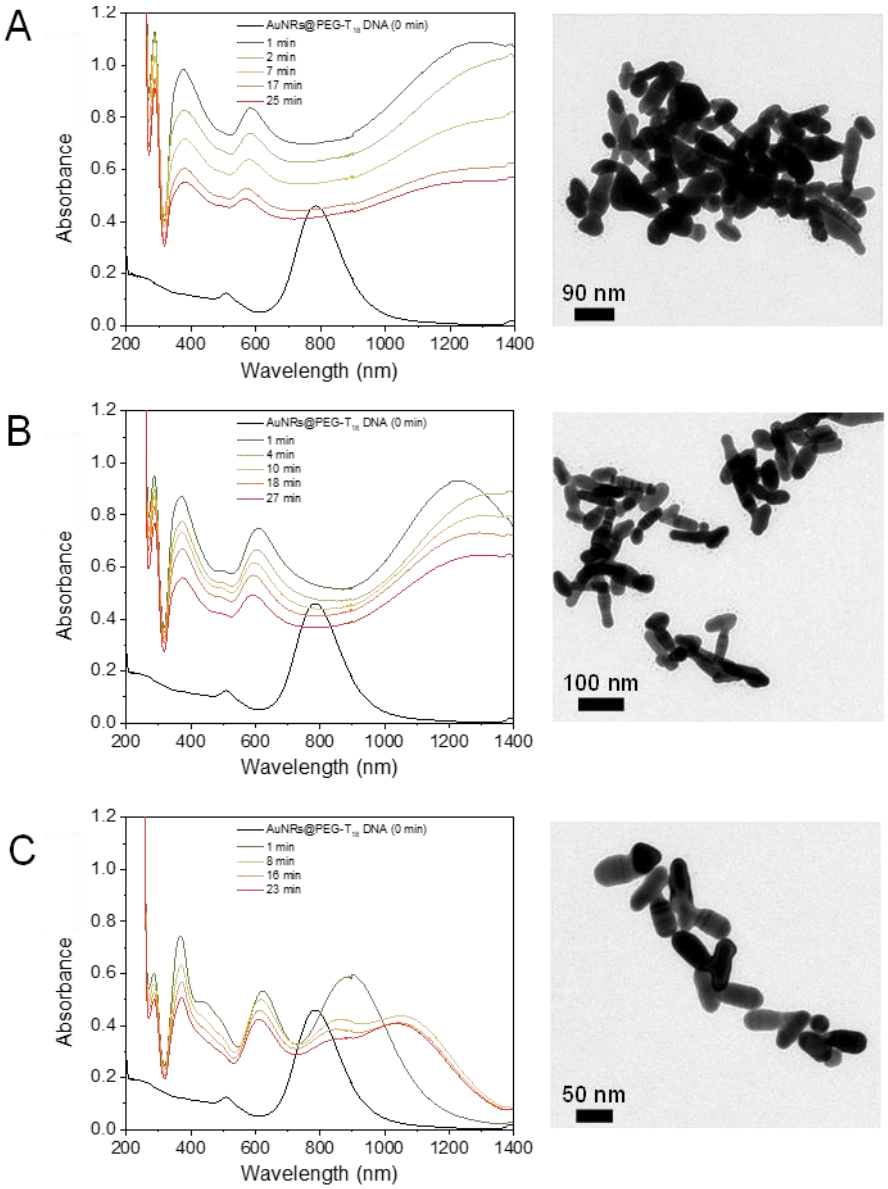

Figure S3. Effect of the [Ag^+]/[Au] ratio during the overgrowth of AuNRs@PEG-T_{18}-DNA (Au NRs length × width = 69 × 18 nm, DNA grafting = 403 strands/AuNR) by means of hydroquinone-assisted Ag^+ reduction in 5 mM phosphate buffer (PB, pH = 7.4). In all cases, the [Au] in the reaction medium was kept at 0.25 mM, and the [HQ]/[Ag^+] ratio to 1. The specific [Ag^+]/[Au] ratios were: (**A**) 9, (**B**) 6, and (**C**) 3. The UV–vis–NIR spectra during each reaction are shown on the left column, and the corresponding TEM micrographs of AuNRs@PEG-T_{18}-DNA@Ag obtained after (**A**) 19 min, (**B**) 20 min, and (**C**) 23 min reaction are shown on the right column. These results show that in none of the cases it was possible to obtain a colloidally stable dispersion of AuNRs@PEG-T_{18}-DNA@Ag. In general, the larger the [Ag^+]/[Au] ratio, the greater the aggregation of the newly formed AuNRs@PEG-T_{18}-DNA@Ag. In all three cases, the reduction kinetics was very fast due to the lack of NaCl in the reaction medium (phosphate buffer was used). This fast kinetics in the absence of NaCl is in agreement with the findings by Lee et al.[1] for PVP/L-SA-assisted Ag^+ reduction (the kinetics gets faster as the [NaCl] in the reaction medium decreases). From (**A**) to (**C**), i.e., with increasing the [Ag^+]/[Au] ratio, we observed that the reduction of Ag^+ ions was also faster. Overall, the very fast Ag^+ reduction kinetics led to uncontrolled overgrowth of AuNRs@PEG-T_{18}-DNA and to their aggregation due to the burial of the stabilizing DNA strands. Moreover, in the absence of NaCl, the DNA charges could not be

efficiently screened. This likely favors the electrostatic attachment of Ag^+ ions on the DNA strands and their preferential reduction therein.

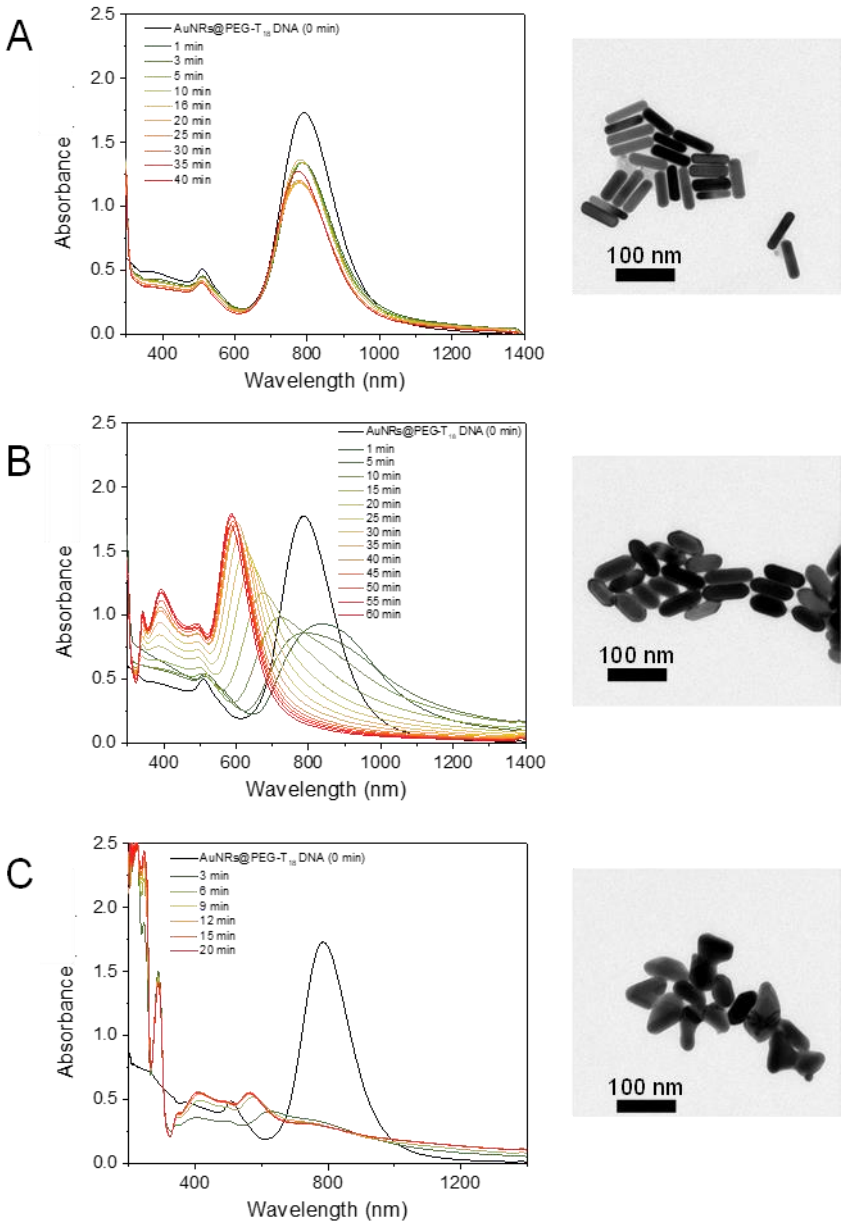

Figure S4. Effect of the concentration of phosphate buffer saline (PBS, pH = 7.4) on the overgrowth of AuNRs@PEG-T_{18}-DNA (Au NRs length × width = 69 × 18 nm, DNA grafting = 403 strands/AuNR) by means of hydroquinone-assisted Ag^+ reduction. The $[Ag^+]/[Au]$ ratio was set to 3 in all experiments, the $[HQ]/[Ag^+]$ ratio was maintained at 1, and the [Au] in the reaction medium was set to 1 mM. The specific PBS conditions were: (**A**) 100 mM PBS containing 1.4 M NaCl, (**B**) 10 mM PBS containing 1.4 M NaCl, and (**C**) 10 mM PBS containing 3 mM NaCl. Note that the PBS concentration refers to the PB concentration, i.e., the sum of the concentrations of HPO_4^{2-} and $H_2PO_4^-$. In (**A**), no Ag overgrowth occurred, due to the strong (almost quantitative) precipitation of Ag_3PO_4 upon addition of $AgNO_3$. For this reason, the optical response of AuNRs@PEG-T_{18}-DNA did not undergo significant changes (almost no Ag^+ was left in the solution to get reduced on their surface, see TEM micrograph in (**A**)). The UV–vis–NIR spectra and TEM micrograph in (**B**) show that a tenfold decrease in PBS concentration significantly minimized, though not fully overcame, this precipitation effect (which was still observed). The results in (**C**) show that maintaining PB concentration at 10 mM (as in (**B**)) while reducing [NaCl] down to 3 mM had a negative impact on the process. Lowering the [NaCl] dramatically altered the kinetics of Ag^+ reduction. It became very fast and, in turn, led to the uncontrolled deposition of silver on AuNRs@PEG-T_{18}-DNA, with no morphological control.

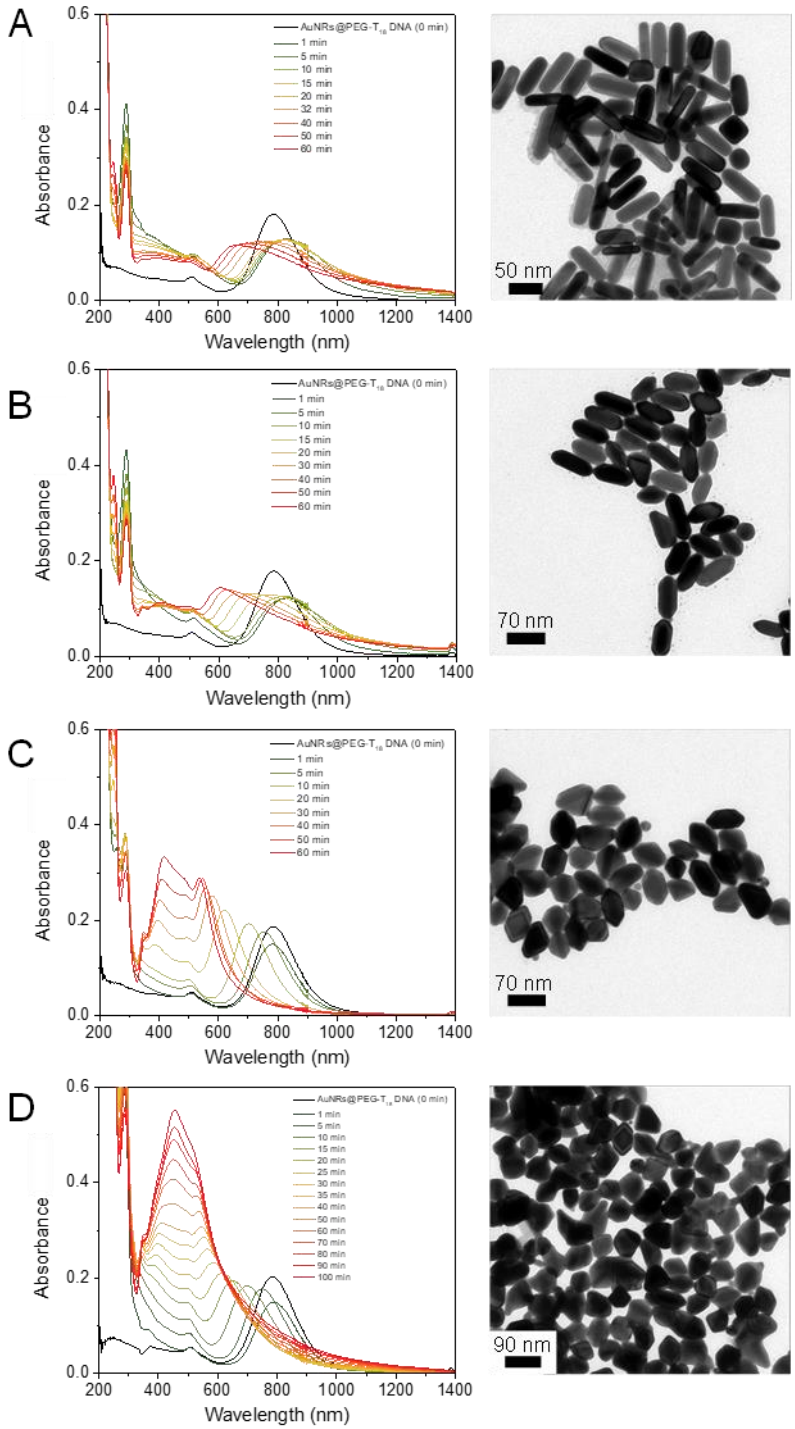

Figure S5. Effect of the concentration of phosphate buffer saline (PBS, pH = 7.4) on the overgrowth of AuNRs@PEG-T18-DNA (Au NRs length × width = 69 × 18 nm, DNA grafting = 403 strands/AuNR) by means of hydroquinone-assisted Ag^+ reduction. The [HQ]/[Ag^+] ratio was kept at 1 in all cases, while the [Au] in the reaction medium was set to 0.1 mM (one time lower than in Figure S4) in order to prevent aggregation. The specific PBS conditions were the following: (**A**) 5 mM PBS containing 0.07 M NaCl, [Ag^+]/[Au] = 3; (**B**) 3 mM PBS containing 0.04 M NaCl, [Ag^+]/[Au] = 3; (C) 1 mM PBS containing 0.014 M NaCl, [Ag^+]/[Au] = 3; and (**D**) 1 mM PBS containing 0.014 M NaCl, [Ag^+]/[Au] = 6. The UV–vis–NIR spectra during silver overgrowth are shown on the left, and the TEM micrographs of AuNRs@PEG-T18-DNA@Ag at the end of each reaction are presented on the right. In general, the lower the PBS concentration, i.e., the lower the concentration of HPO_4^{2-}, $H_2PO_4^-$ and NaCl, the lower the precipitation of Ag_3PO_4. Precipitation was still prominent in (**A**), which drastically reduced the concentration of Ag^+ available in solution for deposition on AuNRs@PEG-T18-DNA. Ag coating is

thicker and more homogeneous in (**B**) as compared to (**A**) and improves significantly in (**C**). Even though epitaxial Ag overgrowth can be appreciated in the TEM micrograph and also in the UV–vis–NIR spectral evolution in (**C**), the quality of the overgrowth was still not fully optimal (asymmetries can be observed). A comparison of the results in (**C**) and (**D**) indicates that an increase of the $[Ag^+]/[Au]$ ratio from 3 to 6 had a negative impact, leading to a loss of shape control.

None of the conditions tested for hydroquinone-assisted Ag^+ reduction in PB and PBS buffer (see e.g., Figure S3–S5) led to a controlled and homogeneous epitaxial Ag deposition on AuNRs@PEG-T_{18}-DNA. This was due to precipitation and kinetic effects associated with the presence of $HPO_4^{2-}/H_2PO_4^-$ and NaCl, respectively. For this reason, PB and PBS buffers are not well suited for the controlled epitaxial overgrowth of Ag on the surface of DNA-functionalized AuNRs. TAE buffers are better suited for this purpose (no precipitation occurs due to the lack of phosphate ions).

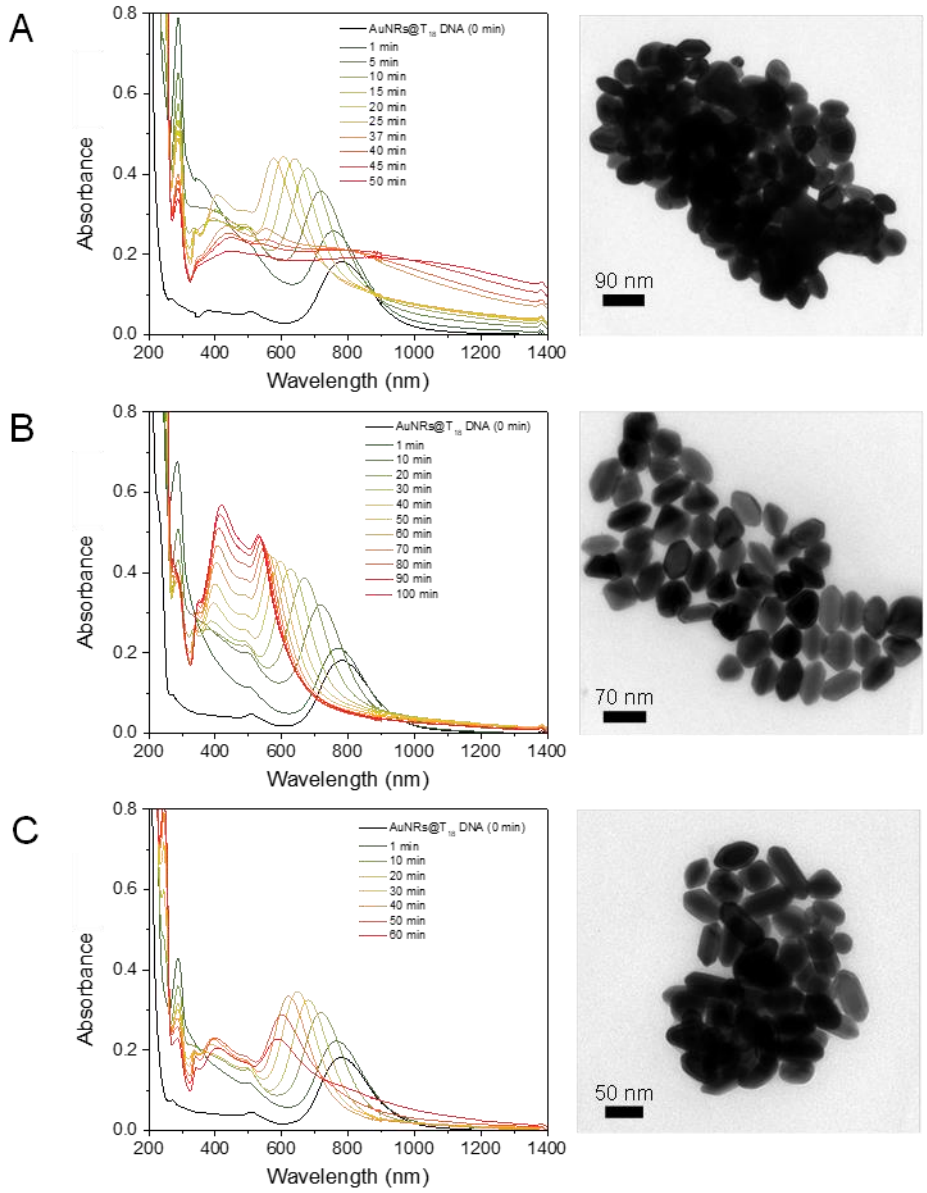

Figure S6. UV–vis–NIR spectra (left column) and corresponding TEM micrographs (right column) of the samples obtained upon hydroquinone-assisted reduction of Ag^+ on AuNRs@T_{18}-DNA (Au NRs length × width = 69 × 18 nm, DNA grafting = 708 strands/AuNR) in TAE buffer (pH = 8) containing Tween 80 and NaCl. The Ag overgrowth conditions were set as follows in all cases: final [Au] in the reaction medium = 0.1 mM, $[Ag^+]/[Au] = 6$, and $[HQ]/[Ag^+] = 1$. The reaction medium consisted of: (**A**) TAE buffer containing 0.001% Tween 80 and [NaCl] = 0.14 M; (**B**) TAE buffer containing 2% Tween

80 and [NaCl] = 0.14 M; and (C) TAE buffer containing 0.001% Tween 80 and [NaCl] = 0.05 M. The comparison of (**A**) and (**B**) shows that an increase of Tween 80 from 0.001% to 2% was needed to prevent the aggregation of the growing AuNRs@T_{18}-DNA@Ag. The comparison of (**A**) and (**C**) shows that a decrease in the [NaCl] from 0.14 M to 0.05 M helped reduce the extent of colloidal aggregation. However, the low amount of Tween 80 in both cases (0.001%) did not suffice to fully stabilize AuNRs@T_{18}-DNA@Ag (see the spectral tail at >700 nm for the 60 min spectrum and the TEM micrograph).

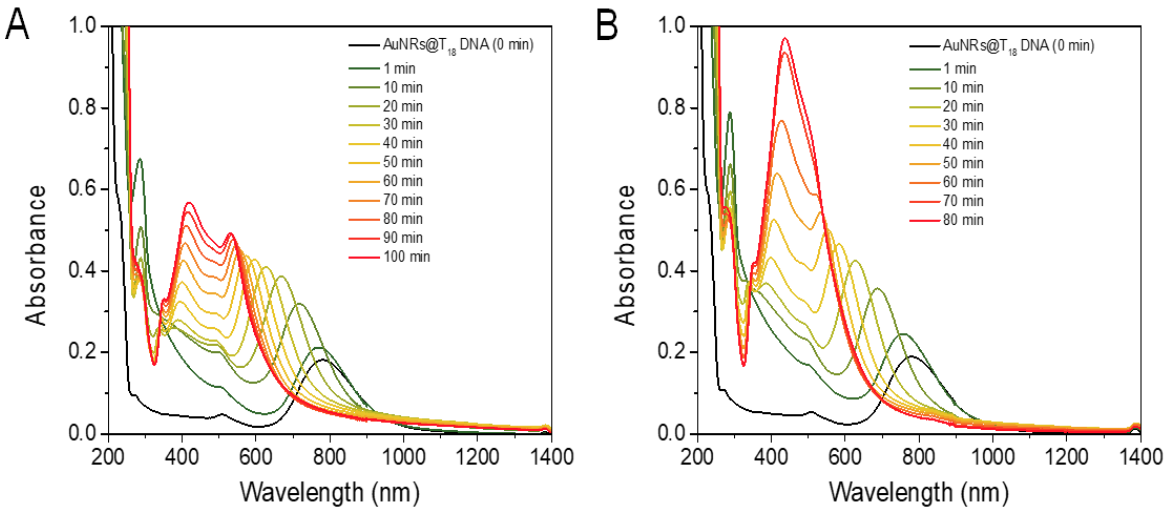

Figure S7. Evolution of the UV–vis–NIR spectra of AuNRs@T_{18}-DNA (Au NRs length × width = 69 × 18 nm, DNA grafting = 708 strands/AuNR) during hydroquinone-assisted reduction of Ag^+ in TAE buffer (pH = 8) containing 2% Tween 80 and two different concentrations of NaCl, while keeping all the other parameters constant (final [Au] in the reaction medium = 0.1 mM, [Ag^+]/[Au] = 6, and [HQ]/[Ag^+] = 1). The reaction medium consisted of: (**A**) TAE buffer containing 2% Tween 80 and [NaCl] = 0.14 M (conditions used in Figure S6B) and (**B**) TAE buffer containing 2% Tween 80 and [NaCl] = 0.05 M. The reaction proceeded faster in 0.05 M NaCl than in 0.14 M. In spite of its faster kinetics, Ag overgrowth was very controlled and uniform. Also at 0.05 M NaCl, the precipitation of AgCl was much lower and, therefore, almost all the added $AgNO_3$ was reduced on the nanorods' surface. This aspect is evident from the UV–vis–NIR spectra: the higher plasmon band intensity at the end of the reaction in (**B**) vs. (**A**) is the result of a minimized loss of Ag^+ ions due to AgCl precipitation (AgCl precipitation was non-negligible in (**A**)).

2. SERS Performance of the Nano-Assemblies.

2.1. Tag-Free SERS Sensing of the dsDNA Interconnecting AuNRs@DNA@Ag and AuNPs@DNA in the Anisotropic Directional Nano-Assemblies

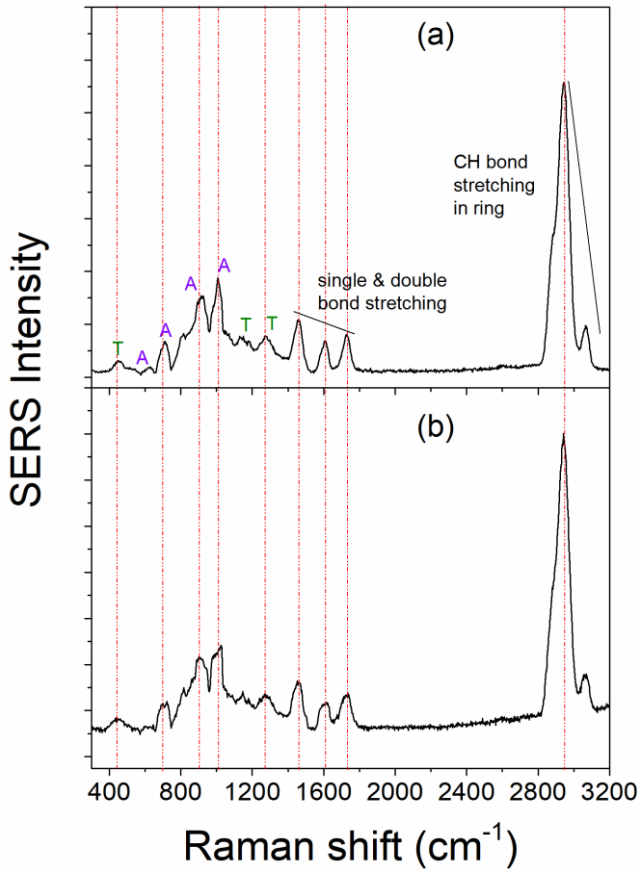

Figure S8. (**a**, **b**) Representative SERS spectra of two individual directional nano-assemblies investigated by DFM-SERS (λ_{laser} = 633 nm). The characteristic SERS peaks from the nucleobases A and T are indicated. These results and the results shown in Figure 5 (main manuscript) confirm that the directional anisotropic nano-assemblies enabled the tag-free detection of the interconnecting dsDNA.

2.2. Calculation of the SERS Detection Limit for dsDNA in the Anisotropic Directional Nano-Assemblies

In the following, we explain how we estimated the lower limit of detection of the interconnecting dsDNA, as provided by the directional nano-assemblies. First, we ensured that the SERS measurements were carried out on individual directional nano-assemblies. This was achieved by ensuring a very low density of directional nano-assemblies on the glass substrate (~ 0.15 per μm^2) and a laser spot size below 1 μm. Second, we assumed that the grafting density of ssDNA (T_{18}-DNA in our case, see Figure 5 in the main text) on AuNRs@DNA and on AuNRs@DNA@Ag remained constant. Therefore, the number of T_{18}-DNA strands that a directional AuNR@T_{18}-DNA@Ag building block had at its tip region was identical to the number of T_{18}-DNA strands that its precursor AuNR@T_{18}-DNA had. Hence, taking into account:

- the average dimensions (from TEM) of AuNRs@T_{18}-DNA: L = 74 nm, W = 21 nm, and tip curvature = 5 nm, and
- their average DNA grafting density of 727 T_{18}-DNA strands/AuNR,

we calculated the surface area of the hemispherically capped AuNRs tip (~438 nm^2) and, thereby, the average number of T_{18}-DNA strands that each AuNR@T_{18}-DNA (and, therefore, a directional AuNR@T_{18}-DNA@Ag) bears at one tip, ~64 ssDNA strands.

We assumed that the assembly of a directional AuNR@T_{18}-DNA@Ag with an AuNP@A_{18}-DNA would lead to the formation of 64 dsDNA at each tip, i.e., assuming all the T_{18}-DNA strands participated in the hybridization.

For the estimation of the limit of detection, we considered the highest population scenario (as shown in figure 3B in the main text) in directional anisotropic nano-assembly formation, that is, that the assembly of one directional AuNR@T_{18}-DNA@Ag building block with AuNPs@A_{18}-DNA would lead to the formation of only one hot spot, i.e., to the assembly of one AuNP@A_{18}-DNA at one tip.

For the calculation, we considered the SERS peak at 1007 cm^{-1}, due to NC stretching in adenine, and established that the intensity of this peak needs to be, at least, twice the noise intensity. That is, only a minimum signal-to-noise (S/N) ratio of 2 would allow to confirm by SERS the presence of adenine, i.e., DNA.

Therefore, the limit of detection LOD =

$$= \text{DNA strands contributing to SERS} \Big/ \left(\frac{I_{1007\ cm^{-1}}}{(Noise\ Intensity) \text{x} \left(minimum\ \frac{S}{N}\ for\ detection \right)} \right) = \quad (1)$$

$$= 64 \Big/ \left(\frac{I_{1007\ cm^{-1}}}{(Noise\ Intensity) \text{x}\ 2} \right) = 64 \Big/ \left(\frac{496255}{(36521) \text{x}\ 2} \right) = 9.4 \quad (2)$$

≅ 10 individual ssDNA

2.3. SERS Sensing of the SYBR-Gold Tagged Directional Anisotropic Nano-Assemblies

We also investigated whether the dsDNA that keeps AuNRs@T_{18}-DNA@Ag and AuNPs@A_{18}-DNA self-assembled in our directional nano-assemblies could incorporate an external Raman tag and, hence, be detected by SERS. This tagged SERS investigation allowed us to determine the enhancement factor provided by the directional nano-assemblies.

As a SERS tag, we used SYBR gold (a cyanine-based dye[2] from Thermo Fischer, Darmstadt, Germany). SYBR gold is known to bind to nucleic acids like dsDNA, ssDNA, and RNA but it mainly intercalates within dsDNA. Figure S9 below shows the Raman spectrum of the dye. The spectrum illustrates that even at a very high concentration (10,000×, provided by the supplier, equivalent to ~19.6 mM [2]), the Raman signal intensities obtained were quite low. As the structure of the dye is proprietary to the company, it is difficult to assign the peaks to the different molecular modes, but similar peak positions have also been reported by Kuhler *et. al.* for SYBR gold.[3]

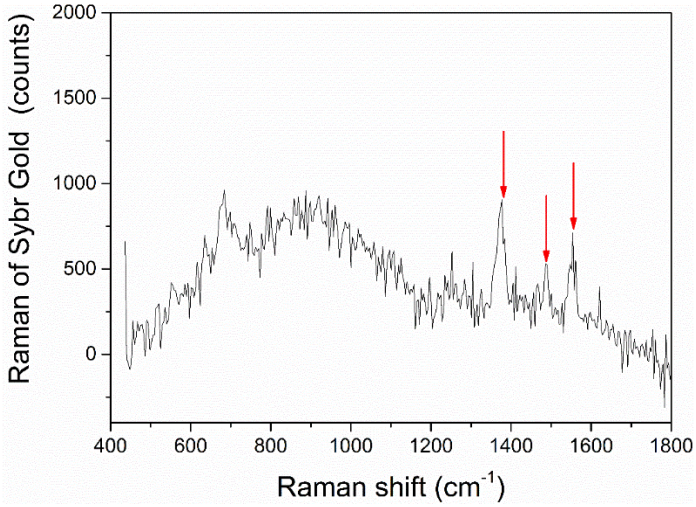

Figure S9. Raman spectrum of SYBR Gold. The red arrows indicate the signature peaks of the molecule at 1373, 1462, and 1556 cm^{-1}.

Representative SERS spectra of single SYBR gold-tagged directional anisotropic nano-assemblies are shown in Figure 6 of the main text and in Figure S10.

Although the Raman cross section of the dye is larger than that of A and T, the SERS intensities of the three are comparable (Figure 6 of the main text and Figure S10). This result suggests that very few dye molecules were located at the hot spot. Indeed, our calculations (see Section 2.4 below) indicated that the maximum dye-to-dsDNA base pair ratio (popularly known as 'dbprs') was ~0.04. This value means that there was ~1 dye molecule for every 25 A–T base pairs. This in our case suggested 2 dye molecules for approximately 3 dsDNA strands.

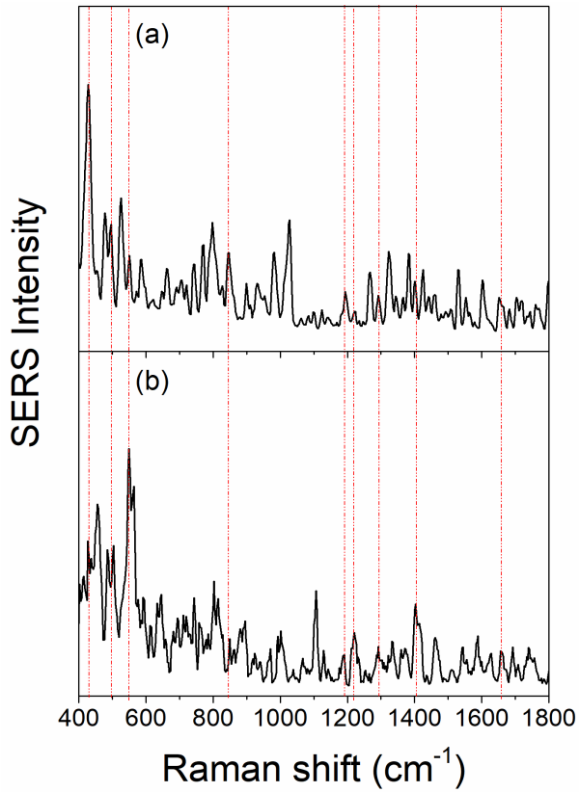

Figure S10. (**a**, **b**) Representative SERS spectra of two SYBR gold-tagged directional nano-assemblies. The red dotted lines showcase a few signature peaks of adenine, thymine, and SYBR gold. The variations in peak intensities and intensity ratio between peaks might be different owing to orientational changes, etc.

2.4. Calculation of the SERS Enhancement Factor of the SYBR Gold-Tagged Directional Nano-Assemblies

Taking into account the calculations in Section 2.2 above, it is possible to assume that the assembly of anisotropic AuNR@T_{18}-DNA@Ag with an AuNP@A_{18}-DNA would lead to the formation of 64 dsDNA at each tip (assuming that all T_{18}-DNA strands participate in the hybridization). Since each dsDNA is formed by 18 base pairs, then, at each tip, there would be 64 × 18 = 1152 base pairs.

Taking into account that the laser spot is ~1 μm in diameter (even though, in reality, it is smaller), then:

$$\text{Laser spot area} = \pi r^2 = \pi \times 0.5^2 = 0.78\ \mu m^2 \quad (3)$$

and the number of SYBR gold molecules present at the laser spot area can be calculated as indicated below:

Original concentration of SYBR gold 10,000× ≡ 19.6 mM

i.e., 1L of 1 M which will contain = 6.023×10^{23} molecules

i.e., 1L of 19.6 mM which will contain = 1.18×10^{22} molecules

To acquire the Raman spectrum of pure SYBR gold, 50 μL of a 19.6 mM SYBR gold solution was spin-coated onto a 24 × 24 mm^2 glass substrate. Thus, the number of SYBR gold molecules in the 0.78 μm^2 laser spot area that provided the pure Raman spectrum was = $(1.18 \times 10^{22}) \times (50 \times 10^{-6}) \times (0.78 \times 10^{-6} \times 10^{-6}) / (24 \times 24 \times 10^3 \times 10^3) = 8 \times 10^8$ molecules, as shown in figure S9. To acquire the SERS signal from the SYBR gold-tagged directional nano-assemblies, we used 30 μL of a 19.6 μM (i.e., 10× solution, added to the nano-assemblies, as mentioned in the main text, materials and methods section) SYBR gold solution, containing $(1.18 \times 10^{22}) \times (30 \times 10^{-6} \times 19.6 \times 10^{-6}) / (1 \times 19.6 \times 10^{-3}) = 3.54 \times 10^{14}$ molecules

Thus, 3.54×10^{14} SYBR gold molecules were present in 100 μL of the final preparation of nano-assemblies. Then, 50 μL of this solution, which thus contained $(3.54 \times 10^{14}) \times (50/100) = 1.77 \times 10^{14}$ molecules, was spin-coated onto the substrate (line 245, main text).

When this amount was spin-coated onto a 24 × 24 mm^2 glass substrate, where only 0.78 μm^2 was the laser spot area, the number of SYBR gold molecules that could occupy the laser spot area, considering a uniform deposition, was $(1.77 \times 10^{14}) \times (0.78 \times 10^{-6} \times 10^{-6}) / (24 \times 24 \times 10^3 \times 10^3) = 2.37 \times 10^5 \cong 2.4 \times 10^5$ molecules

Thus, the number of SYBR gold molecules present in the laser spot area was ~2.4×10^5.

Considering that the hot-spot area was determined by the AuNR cap radius (10.5 nm) and the radius of AuNP@A_{18}-DNA (7.5 nm), then:

Maximum hot-spot area = 153 nm^2

hence: total dye molecules per hot spot =

= (SYBR gold molecules in laser spot) × (hot-spot area/laser spot area)

$= (2.4 \times 10^5) \times [(153 \times (10^{-9})^2] / [0.78 \times (10^{-6})^2] \cong 47$

Therefore, the maximum dye-to-base pair ratio (dbprs) was 47 / 1152 ≅ 0.04

and the average enhancement factor (EF) was $(I_{SERS}/I_{Raman}) \times (N_{Raman}/N_{SERS})$,

$EF_{@1373cm^{-1}} = 1.53 \times 10^8$

$EF_{@1462cm^{-1}} = 1.65 \times 10^8$

Therefore, the SERS EF of the anisotropic directional SYBR gold-tagged nano-assemblies was ≅ 1.6×10^8.

References

1 Lee, J.H.; Kim, G.H.; Nam, J.M., Directional synthesis and assembly of bimetallic nanosnowmen with DNA. *J Am Chem Soc* **2012**, *134*, 5456–5459.

2 Zipper, H.; Brunner, H.; Bernhagen, J.; Vitzthum, F., Investigations on DNA intercalation and surface binding by SYBR Green I, its structure determination and methodological implications. *Nucleic Acids Res* **2004,** *32*, e103.

3 Kuhler, P.; Roller, E.M.; Schreiber, R.; Liedl, T.; Lohmuller, T.; Feldmann, J., Plasmonic DNA-origami nanoantennas for surface-enhanced Raman spectroscopy. *Nano Lett* **2014**, *14*, 2914–2919.